PCCP

Accepted Manuscript

This is an *Accepted Manuscript*, which has been through the Royal Society of Chemistry peer review process and has been accepted for publication.

Accepted Manuscripts are published online shortly after acceptance, before technical editing, formatting and proof reading. Using this free service, authors can make their results available to the community, in citable form, before we publish the edited article. We will replace this *Accepted Manuscript* with the edited and formatted *Advance Article* as soon as it is available.

You can find more information about *Accepted Manuscripts* in the Information for Authors.

Please note that technical editing may introduce minor changes to the text and/or graphics, which may alter content. The journal's standard Terms & Conditions and the Ethical guidelines still apply. In no event shall the Royal Society of Chemistry be held responsible for any errors or omissions in this *Accepted Manuscript* or any consequences arising from the use of any information it contains.

ROYAL SOCIETY OF CHEMISTRY

www.rsc.org/pccp

Real time observation of the excimer formation dynamics of gas phase benzene dimer by picosecond pump-probe spectroscopy

Mitsuhiko Miyazaki and Masaaki Fujii*

Chemical Spectroscopy Division, Chemical Resources Laboratory, Tokyo Institute of Technology, 4259-R1-15, Nagatsuta-cho, Midori-ku, Yokohama-shi, 226-8503, Japan.

email: mfujii@res.titech.ac.jp

Abstract

We observed the real-time excimer (EXC) formation dynamics of a gas phase benzene dimer (Bz_2) cluster after photo-excitations to the S_1 state by applying an ionization detected picosecond transient absorption method for probing the visible EXC absorption for the first time. The time evolution of the EXC absorption from the S_1 0^0 level shows a rise that is well fitted by a single exponential function with a time constant of 18 ± 2 ps. The structure of the Bz dimer has a T-shape structure in the ground electronic state, and that in the EXC state is a parallel sandwich (SW) structure. Thus, the observed rise time corresponds to the structural change from the T to the SW structures, which directly shows the EXC formation. On the other hand, the EXC formation after excitation of the S_1 6^1 vibrational level of the stem site showed a faster rise of the time constant of 10 ± 2 ps. Supposing equilibrium between the EXC and the local excited states, it followed that the intramolecular vibrational energy redistribution rate of the 6^1 level is largely enhanced and becomes faster than the EXC formation reaction.

Physical Chemistry Chemical Physics Accepted Manuscript

1. Introduction

An excimer (EXC) is a complex including an excited molecule. Its characteristic optical properties have been used in various applications, such as lasers,[1] a probe for contact between aromatic parts including biological system,[2, 3] and so on. The reaction dynamics of the excimer (EXC) formation of aromatic systems has attracted attention as one of the characteristic reactions in electronic excited states in neat liquids, crystals, and even in DNAs.[4-17] Recently, EXC has become important in photovoltaics because it is a precursor of a triplet pair by singlet fission, which enhances the efficiency of a solar cell significantly.[18-21] Such EXC formation can be clearly detected by the fluorescence spectrum. The fluorescence spectrum of aromatic systems is largely red-shifted and broadened in comparison to that of the monomer when aromatic rings are closely in contact with each other, though the corresponding absorption keeps the same feature as that of the monomer.[2, 3] This fluorescence is the characteristic feature of EXC, which is called EXC fluorescence. The carrier of the EXC fluorescence has been assigned to an excited state of the aromatic dimer that is formed by dimerization of the photo-excited monomer with a normal monomer.

From the language of quantum chemistry, such an EXC state is explained by the idea of a resonance of the excitation between two equivalent molecular sites.[2, 22-27] In the excited state of a homo-dimer, two indistinguishable local excited (LE) states, $\phi_1^*\phi_2$ and $\phi_1\phi_2^*$, are possible, where $\phi_1^*\phi_2$ and $\phi_1\phi_2^*$ represent excited states such that only the site 1 is excited and vice versa. In such cases, linear combinations are required to describe the excited state as $\Psi_{\pm}(\mathrm{EXC}) = \phi_1^*\phi_2 \pm \phi_1\phi_2^*$. (Formally, ion-paired states, $\phi_1^+\phi_2^- \pm \phi_1^-\phi_2^+$, may also contribute to the EXC state, though their contribution has been discussed by mainly theoretical studies.[2, 28, 29]) As usual, one of the combinations results in a bound intermolecular potential and the other repulsive.

Since, in the case of aromatic dimers, this resonance is caused by the excitation of electrons in the π orbitals, which results in an exchange of the excitation between them, a much stronger interaction is expected when the π orbitals of the two molecules have larger overlaps. Therefore, a face-to-face, parallel sandwich (SW) structure has been believed to exist for aromatic EXC states.[2] On the other hand, usually two types of structures are thought to be the structure of aromatic dimers in the ground state: one is the SW structure, which is similar to that expected for the EXC; the other is a T-shape structure in which a CH bond of one ring sticks on the π cloud of the other.[30-34] In the latter case, the π orbitals are orthogonal, and no EXC interaction is exerted. Thus, when the ground state has the T-shape structure, a drastic structural change from T to SW is expected, associated with the EXC formation, while no significant change after photoexcitation will take place if the ground state has the SW structure.

Clusters produced in a supersonic jet expansion provide us an opportunity to observe the dynamics starting from a well-defined initial structure without any perturbations from solvent molecules. The advantage of the molecular clusters for studying the dynamics has been demonstrated on many systems.[35, 36] However, real-time observations of EXC formation dynamics in gas phase have not been reported, except for fluorene and dibenzofuran dimers. Saigusa and Lim have reported that both of the EXC states were formed ~40 ps after their photo-excitation from a picosecond fluorescence depletion detected pump-probe spectroscopy.[37] The problem of this report was that the fluorene dimer and the dibenzofuran dimer are

Physical Chemistry Chemical Physics Accepted Manuscript

thought to have significantly different structures in spite of the same EXC formation lifetime. The fluorescence excitation spectrum of the fluorene dimer shows sharply structured bands, while that of dibenzofuran is completely broadened upon dimer formation. This contrast in the spectral feature had been explained by the extent to which the excited state couples with the EXC state i.e. a structural similarity to EXC. Thus the SW structure and much faster EXC formation were expected for dibenzofuran, because the SW structure is usually assumed for aromatic EXCs. In fact, the parallel stacked pyrene crystal converts to the EXC with a 140 fs upon excitation.[16] Thus almost the same EXC formation rate for both the systems obtained by Saigusa and Lim has suggested some doubt concerning the simple relation between the bandwidth of the absorption spectra and the cluster structure of the aromatic dimers, and also the EXC formation mechanism. Therefore, a study on a system with definite structure is desired.

In this sense, the benzene dimer (Bz_2) is very important, because it is the only aromatic dimer for which the EXC formation has been confirmed, and the structure is surely determined in both the S_0 and S_1 (EXC) states in the gas phase. The structure of Bz_2 on the electronic ground state has been thoroughly investigated for a long time due to the fundamental importance as the simplest model of aromatic-aromatic interactions. Experimentally, only the T-shape dimer has been observed in the gas phase,[38-44] while both the T and SW structures have been proposed by quantum chemical calculations with nearly identical stabilization energies.[30-34] The clusters of Bz in the gas phase was reported by Shinohara and Nishi via the S_2 excited state, and the EXC formation was suggested.[45] However, they did not show any direct spectroscopic evidence of EXC formation, and their reported lifetime in nanosecond order was not consistent to a 100 ps lifetime measured by Radloff et al.[46] The EXC formation of the Bz_2 in the gas phase cluster was first confirmed by Hirata *et al*. by measuring the dispersed fluorescence and photodissociation spectra of the S_1 state.[47, 48] They showed that the S_1 0^0 level emits only red-shifted broad fluorescence centered at around 310 nm (32249 cm^{-1}, 3.9984 eV), which matches with EXC fluorescence observed in the solution phase. The photo-dissociation spectrum of the S_1 0^0 level shows a broad absorption centered at around 460 nm (21733 cm^{-1}, 2.6946 eV), which again well corresponds to the EXC absorption observed in liquid benzene.[14, 17] Recent quantum chemical calculations have ascribed the absorption to a transition from the S_1 EXC state to the dissociative EXC state formed from of the S_3 excited state and the S_0 state of Bz. Hereafter, we will call it EXC absorption.[49-54] According to the observation, they concluded that the S_1 0^0 level undergoes the EXC formation reaction without an activation barrier.[47, 48] The structure in the EXC state was commonly accepted as the SW structure based on theoretical works and experimental estimations.[2, 49-57] Therefore, in the course of the EXC formation, the locally excited (LE) T-shape Bz_2 must be followed by a ring rotation motion to face the Bz rings leading to the SW-shaped EXC. The S_1 6^1 level, on the other hand, shows a dual fluorescence: one is the EXC fluorescence and the other is structured emission around 275 nm (36353 cm^{-1}, 4.5072 eV).[47, 48] The structured emission is attributed to emission from the LE state, where the excitation is localized on one benzene ring, according to the time evolutions of the photodissociation yield measured at 500 nm (19994 cm^{-1}, 2.4790 eV) of the EXC absorption probing the LE and EXC fluorescence. In addition, since both of the time evolutions give the same time dependence, they concluded that the LE and EXC states

Physical Chemistry Chemical Physics Accepted Manuscript

interchange in the timescale faster than the nanosecond laser pulses used.

The EXC formation dynamics of Bz was first studied in the liquid phase.[11, 12, 14, 17, 58, 59] The EXC absorption decays with a lifetime of about 28 ns, corresponding to the lifetime of the EXC state in liquid Bz.[11, 58, 59] The dynamics has also been studied by applying pump-probe spectroscopy while utilizing ultrafast laser pulses. From the time evolutions of the absorbance at 420 nm (23802.8 cm^{-1}, 2.9512 eV) triggered by a 355 nm (28161 cm^{-1}, 3.4915 eV) or 266 nm (37582.8 cm^{-1}, 4.6597 eV) excitation of a neat Bz liquid, Miyasaka *et al.* reported that the EXC formation was represented by a time constant of 12−20 ps.[14] Inokuchi *et al.* observed a slow rising component with a time constant of 14 ps that appeared at 580 nm (17237 cm^{-1}, 2.1371 eV) after 268 nm (37302 cm^{-1}, 4.6249 eV) pumping, as a part of their study on ionization dynamics of liquid Bz using 100 fs pulses, and attributed it to the EXC formation.[12] However, from the view point of structurally specified dynamics, the dynamics study in the liquid phase has disadvantage concerning the distributions in the initial mutual orientation around the excited molecules and solvent-solute interactions.

The real-time observation has not yet been applied to the gas phase Bz_2. Now, one can deduce the relation between the structure and the EXC formation dynamics from time-resolved spectroscopy on this structurally well-defined system. In the present work, we will apply an ionization detected picosecond pump-probe spectroscopy to a gas phase Bz_2 cluster so as to investigate the EXC formation reaction dynamics in real time.

2. Experiment

Figure 1 shows the excitation scheme of the measurement. The experiment was based on a picosecond transient absorption spectroscopy of supersonically cooled Bz_2. The dynamics of EXC formation can be traced by monitoring the time evolution of the EXC absorption intensity after photo-excitation, because the visible absorption of the excited state is recognized as a signature of EXC formation. The absorption of visible light is measured by the depletion of the Bz_2^+ signal.

At first, Bz_2 is resonantly excited to the S_1 0^0 or S_1 6^1 level by the excitation laser, ν_{exc}. After a long time delay (few tenths of a nanosecond), an ionization laser, ν_{ion}, ionizes the excited species and the population is monitored as Bz_2^+. The signal intensity is proportional to the S_1 state population of Bz_2. Under this condition, a dissociation laser, ν_{diss}, is introduced with a variable delay time of Δt from ν_{exc}. The wavelength of ν_{diss} is resonant with the EXC absorption so as to dissociate EXC formed. This leads to a depletion of the monitored ion signal. The larger is the percentage of EXC in the excited state, the larger is the dissociation of the cluster; that is, the deeper is the depletion. Therefore, by monitoring the amount of depletion as a function of the delay time, the time evolution of the EXC state can be traced. The time evolution is converted to the population change by taking the logarithm of the depletion. This scheme is similar to what we have applied to phenol–$(NH_3)_n$ clusters to observe the dynamics of the excited-state hydrogen-transfer reaction.[60, 61]

Pulsed picosecond lasers were equipped for ν_{exc} and ν_{diss} to trace the fast dynamics, while a nanosecond pulse was used as ν_{ion}. A second harmonic of a regeneratively amplified Ti/S laser (~13 mJ/pulse) was separated into two beams, which pumped two tunable OPO/OPA systems (TOPAS, Light Conversion). One

Physical Chemistry Chemical Physics Accepted Manuscript

signal output was frequency doubled, and was used as ν_{exc}; the signal output of the other system was used as ν_{diss}. The second-harmonic output of a Nd^{3+}:YAG laser (INDI 10, Spectra Physics) pumped dye laser (Cobra Stretch, Sirah) was used as ν_{ion}. ν_{exc} and ν_{diss} were coaxially introduced into a vacuum chamber after adjusting the delay time and the focal points by delay stages and telescopes. ν_{ion} was introduced in a coaxial, but counter propagating, manner to the ps pulses. All of the lasers were focused on a jet expansion by quart lenses with f = 250 mm. The wavelength of ν_{exc} was set to the 0^0_0 (38042 cm^{-1}, 4.7166 eV, 262.79 nm) or 6^1_0 (38563 cm^{-1}, 4.7812 eV, 259.24 nm) transitions of Bz_2 (stem),[56, 62-65] and ν_{diss} was set to 475 nm (21047 cm^{-1}, 2.6095 eV), which is the center of the EXC absorption.[11, 14, 17, 58, 59] The wavelength of ν_{ion} was set to 270 nm (37026 cm^{-1}, 4.5907 eV), which was determined from a compromise between the signal intensity and the excess energy of the resultant cation. From autocorrelation measurements, the pulse widths of both picosecond pulses were about 3 ps. The instrumental function was also checked by the time evolution of 1+2' ionization of the 6^1_0 transition of bare benzene. In this measurement, the benzene cation intensity was monitored as a function of the delay time between ν_{exc} and ν_{diss}, which in this case worked as the ionization laser. The energy resolution of ν_{exc}, estimated from the band width of 6^1_0 transition of bare benzene, was about 15 cm^{-1} (0.0019 eV) in FWHM. The intensity of ν_{diss} was adjusted by checking the linearity of the depletion so as not to saturate the EXC absorption, and was set to about 300 nJ/pulse. Then, the depletion of ion signal was 20–30%.

Benzene was diluted in Ne gas (2 bars), and was expanded into a vacuum chamber through an orifice (dia. 0.8 mm) of a pulsed valve (General valve, series 9) to form Bz_2 in the supersonic jet expansion. The sample was cooled to −25 °C so as to reduce the vapor pressure and contributions from higher clusters. The temperature of the jet expansion, estimated from the rotational contour analysis of the 6^1_0 transition of benzene monomer, was about 1.5 K. The jet expansion was interacted by laser pulses in front of a quadrupole mass filter, and the resultant ions were bent 90 degrees by an electrostatic field, and then introduced into the mass filter. The Bz_2 (or Bz monomer) cation was detected mass selectively by a channeltron-type ion detector, followed by a current amplifier.[66] The ion signal was averaged by a boxcar integrator and stored in a personal computer.

3. Results

3-1. Resonance enhanced 2 photon ionization spectra

Figure 2 (a) shows the 1+1 resonance enhanced 2 photon ionization spectra of Bz_2. The upper and lower traces represent spectra recorded by using picosecond and nanosecond lasers, respectively. Though the spectrum obtained by the picosecond laser is broadened due to the spectral resolution of the picosecond pulse (~15 cm^{-1}, 0.0019 eV), it well corresponds to the nanosecond spectrum, and no extra band appears. Four bands at 38042, 38563, 38966, and 39490 cm^{-1} well correspond to previous reports and are assigned to the 0^0_0, 6^1_0, 1^1_0 and $6^1_0 1^1_0$ transitions, respectively.[56, 62-65] The 0^0_0 and 1^1_0 transitions, which are forbidden in the monomer, are weakly allowed due to the symmetry reduction of the stem site in the T-shape dimer. A hole-burning spectroscopy on the C_6H_6–C_6D_6 mixed dimer by Scherzer *et al.* has confirmed that the excitation of the transitions was localized on the stem site of the T-shape dimer.[44] Weak bands on the blue

Physical Chemistry Chemical Physics Accepted Manuscript

side of the 6^1_0 (stem) band have been assigned to the progression of the intermolecular vibration built on the 6^1_0 transitions localized on the top site of the dimer.[40, 44] The appearance of the intermolecular vibrational bands suggests that the electronic excitation on the top site causes a change in the intermolecular geometry. In contrast, the excitation of the stem site does not produce any significant geometrical change because of the lack of intermolecular bands. The π cloud of the top site interacts with the partner, but that of the stem site does not. This difference would cause the sharp difference of the intermolecular vibrational bands. The transitions of higher clusters (mainly trimer and tetramer), which are expected on the red side of the 6^1_0 (stem) band due to fragmentations in the ionic states, have not been observed under this condition.[67-69] Similarly, hot band transitions of the dimer do not appear in this region. Thus, under this condition, the vibrational degrees of freedom were efficiently cooled down to the ground state, and higher clusters did not contaminate into the carrier of EXC signal. It should be noted that no visible emission was observed from UV-excited Bz_3 and Bz_4. This observation was interpreted as indicating the lack of EXC formation in Bz_3 and Bz_4.[47] Thus, we can omit the contribution of the trimer and the tetramer for the EXC signal. The time evolutions of the EXC absorption were measured under this condition by fixing the excitation laser at positions indicated by arrows in Fig. 2.

3-2. Time evolutions of the EXC absorption

Figure 3 (a) and (b) show the time profiles of the EXC absorption after excitations to the S_1 0^0 and S_1 6^1 (stem) levels, respectively. Fig. 3 (c) shows the time profile of the 1+2' REMPI signal of the 6^1_0 transition of the benzene monomer, which is well represented by a step function convoluted with a 3.1 ps FWHM Gaussian, and can be regarded as being the instrumental function of our system. The EXC absorption apparently shows slow rises compared to the instrumental function. Thus, the depletion of the signal is safely ascribed to the EXC formation dynamics. The depletions reach the maximum at around 100 ps and 50 ps for the 0^0 and 6^1 excitations, respectively, and then are kept constant up to 200 ps. The depletion for the 0^0 excitation was slightly deeper than that for the 6^1 excitation. This observation is in line with a pump-probe fluorescence depletion study by Hirata *et al.*[47] They reported that the depletion efficiency of the EXC absorption decreases as the excitation energy increases. These observations imply that the efficiency of the reaction decreases with the vibrational excitation.

The rising time of the EXC absorptions was estimated by a single exponential fitting in which the instrumental function parameters were constrained to the value obtained from the 1+2' ionization of the monomer 6^1 level. The best-fitted functions are appended on each time profile in Fig. 3 as black curves. The obtained time constants were 18 ± 2 and 10 ± 2 ps for the 0^0 and 6^1 excitations, respectively. The rising time of the EXC absorption after the 6^1_0 excitation is about two-times faster than that of the 0^0 excitation in spite of the low reaction yield.

4. Discussions

4-1. Intermolecular vibrations and the reaction coordinate

In general, a molecular dimer has six intermolecular coordinates. Figure 4 shows these intermolecular

Physical Chemistry Chemical Physics Accepted Manuscript

motions schematically. The EXC formation follows a reaction coordinate that connects from the T- to the SW-shapes. The reaction coordinate is considered to consist mainly of torsional vibration of the two rings and intermolecular stretching vibrations, because the main differences between the T and SW structures are in the angles of the molecular planes and the intermolecular distance. In the SW-shape, the two torsional vibrations are equivalent and degenerate due to the symmetry.

The out-of-plane bending vibration may couple with the torsional vibrations by the relative motion to conserve the center of mass. On the other hand, the in-plane bending vibrations of the T-shape are independent from the reaction coordinate. In the SW-shape these vibrations may weakly couple with the reaction coordinate by conservation of the center of mass. The in-plane bending vibrations are also degenerate in the SW-shape.

The in-plane rotations of both the T- and SW-shapes are almost free rotation, and are independent from the reaction coordinate. Higher vibrational levels of such an internal rotation correspond to large angular momentum states, which usually have poor Franck-Condon overlaps between rotation-less states. The temperature of the molecular beam in this study was low enough to cool down the internal rotation, and thus the initial state of the reaction should be nearly the vibrational ground state of the in-plane rotation.

Within the six intermolecular vibrations, only the in-plane rotations of both structures and in-plane bending of the T-shape are independent from the reaction coordinate. However, all of the others may contribute to the reaction coordinate. The T-shape structure has only one torsional vibration, but the SW-shape has two degenerate torsional vibrations. That is, the coefficients of the linear combination of the reaction coordinate are largely altered as the reaction proceeds. This means that the reaction and the intramolecular vibrational energy redistribution (IVR) into the intermolecular vibrations cannot be separated in this reaction.

4-2. Time evolutions and the EXC formation mechanism

4-2 (a) 0^0 excitation

Although the initial LE state in the 0^0 excitation has no excess energy, the EXC absorption shows the rise with the time constant of 18 ps. This means that the reaction has no barrier on the coordinate. As mentioned above, the reaction coordinate and bath modes interchange with each other in this system, and conservation of all the energy on the reaction coordinate is improbable. The back reaction from the EXC to LE state, however, needs the conservation of all the energy on the reaction coordinate. The IVR in the EXC cannot be avoided because of the 4000 cm^{-1} (0.496 eV) energy difference between LE and EXC.[29, 49, 51-54] Thus, the reaction should be represented by the one sided first order reaction from the LE to the EXC states (see Fig. 5). The IR spectrum in the S_1 state after $S_1 0^0$ excitation has shown that only the SW-shaped EXC exclusively exists.[70] This is also consistent with the present observation that the time evolution can be fitted by the single exponential function. The obtained time constant of 18 ps, therefore, should represent the EXC formation time constant. Because the structure of the ground state Bz_2 is the T-shape, this time constant corresponds to the structural change to the SW-shape. This is the second example of determining the time constant of the gas phase EXC formation following dibenzofuran and fluorene dimers.[37]

Physical Chemistry Chemical Physics Accepted Manuscript

The rotational constant around the A and B axis of Bz is 5.7 GHz.[71] From this value, the classical period of rotation of ~100 ps is estimated from the inverse of the rotation constant. A quarter rotation is sufficient to convert the LE state (T-shape) into the SW-shaped EXC. The observed EXC formation time constant of 18 ps is about 1/5 of the rotational period of Bz. Thus, the reaction rate is similar to or a little faster than the period needed for classical quarter rotation. Saigusa and Lim reported time constants of 36 and 46 ps for fluorene and dibenzofuran, which are tricyclic aromatics, respectively. Though the EXC interaction is expected to be stronger in the tricyclic systems because of the larger polarizabilities, the reactions are slower than that of benzene (18 ps). The heavier mass of these molecules (166 u and 168 u) may account for a part of the slow rate. In these systems, however, the rotation period of 200–800 ps, depending on the rotation axes, are estimated from the rotational constants.[72, 73] Therefore, the ratio of the reaction and rotational times are again about 1/5 in these molecules. These suggest that the EXC formation dynamics is close to the free rotation of a corresponding monomer.

The S_1 origin of Bz_2 shows a small splitting of about 1.5 cm^{-1}.[47, 64] No definite explanation has been given yet. An exciton splitting between equivalent sites has been intuitively imagined as the simplest explanation. But now the nonequivalence of two benzene rings in the ground state dimer seems to be established, and also the transition dipoles may not interact with each other in the T-shaped geometry. Other experimental results have also provided negative signs.[40, 47] A tunneling site interchange of the top and stem sites has been suggested as an alternative by Henson *et al*. because of the low barrier height separating the reaction path (only 100 cm^{-1} (0.0124 eV) by a sophisticated *ab initio* calculation).[31, 40] The tunneling causes splitting in both the ground and excited states, and the allowed transitions between them may explain the observed splitting in the 0^0 band. These two scenarios would be distinguished by observing the real-time dynamics subsequent to a coherent excitation of the 0^0 band, as they have already suggested.[31, 40] If the exciton interaction is valid, a quantum beat with few tenths of a picosecond may be observed in the dynamics, because the two transitions with the common level in the ground state are coherently excited. In the case of the site interchange, on the other hand, such beat should not be observed because the levels in the ground state are not common. The time profile in the present study could not detect such a beat within our signal-to-noise ratio. This observation would support the tunneling splitting mechanism.

4-2 (b) 6^1 excitation of the stem site

The observed rise time of the EXC absorption is 10 ps for the 6^1 level. The reaction is accelerated by about two times compared to that from the 0^0 excitation, 18 ps. In the zeroth-order approximation the 6^1 vibration is localized in the stem site, and is independent from the reaction coordinate of the EXC formation. Thus, the acceleration means that the vibrational energy of 6^1 is transferred to the reaction coordinate by IVR. Here, the IVR rate of the 6^1 level must be faster than or at least comparable to the EXC formation rate. If so, the IVR rate in the dimer is ~8000-times faster than that in the monomer (87 ns).[74] Though mode 6 is a degenerate vibration in the monomer, it splits into 6a and 6b modes in the stem site of the T-shape. The symmetry of the 6a mode becomes totally symmetric, and is the same as the intermolecular stretching, and that of the 6b mode belongs to the same symmetry as the in-plane intermolecular bending in the T-shape,

Physical Chemistry Chemical Physics Accepted Manuscript

which is perpendicular to the reaction coordinate. Thus, the IVR from the 6a mode will accelerate the EXC formation, while the 6b mode does not contribute directly.

Hirata *et al.* have reported that the 6^1_0 excitation emits the LE fluorescence in addition to the EXC fluorescence, and that the lifetime and the photodissociation yields measured by monitoring each emission are the same as the EXC fluorescence.[47] This observation means the existence of equilibrium faster than the nanosecond time scale. To achieve such a fast equilibrium, sufficient energy to be able to overcome the energy difference between the LE and EXC states must remain in the reaction coordinate. As well as the 0^0 excitation, the IVR in the EXC state should take place. Thus, the IVR in the EXC state must have sufficient selectivity not to lose the energy (more than 521 cm^{-1} (0.0646 eV)) from the intermolecular modes that contribute to the reaction coordinate. The intermolecular vibrational modes that are isolated from the reaction coordinate are in-plane and out-of-plane rotations in the T-shape, in-plane bending in the T-shape and in-plane rotation in SW. Three of these modes are rotational motions that have angular momenta. Thus, the IVR to these rotational modes corresponds to the rotational excitation, and therefore must couple with the whole rotation of the dimer because of conservation of the total angular momentum. Such a restriction would be the reason why the coupling to these modes is weak.

Based on this consideration, we propose the following simple reaction model, which is sketched in Fig. 5, to explain the time evolution of the 6^1 level. The initial 6^1 level decays with two reaction paths: one is a direct reaction to the EXC state; the other is the IVR within LE. The EXC generated from LE 6^1 immediately relaxes to the higher vibrational states of EXC by IVR. The higher vibrational states of EXC and the vibrationally excited states in LE are in equilibrium with each other, based on dispersed fluorescence spectroscopy.[47] The reaction rate of the direct reaction from the 6^1 level to EXC without IVR should be the same as that from the 0^0 level. The rate constants of the forward and back reactions between EXC and LE have been reported to be the same based on fluorescence depletion experiments by Hirata *et al*.[47] Therefore, the rate equation of each state and the solutions are given as follows under the initial condition of the selective excitation of the 6^1 level, [LE](t = 0) = 1:

$$\frac{\mathrm{d[LE]}}{\mathrm{d}t} = -(k^+ + k_{IVR})\,[\mathrm{LE}], \tag{1}$$

$$\frac{\mathrm{d[EXC]}}{\mathrm{d}t} = k^+\,[\mathrm{LE}] - k_{EQ}\,[\mathrm{EXC}] + k_{EQ}\,[\mathrm{LE_{IVR}}], \tag{2}$$

$$\frac{\mathrm{d[LE_{IVR}]}}{\mathrm{d}t} = k_{IVR}\,[\mathrm{LE}] + k_{EQ}\,[\mathrm{EXC}] - k_{EQ}\,[\mathrm{LE_{IVR}}], \tag{3}$$

$$[\mathrm{LE}](t) = \exp(-(k^+ + k_{IVR})\,t), \tag{4}$$

$$[\mathrm{EXC}](t) = \frac{(k^+ - k_{EQ})}{(k^+ + k_{IVR} - 2\,k_{EQ})}[1 - exp(-(k^+ + k_{IVR})\,t)] + \frac{(k_{IVR} + k^+)}{2\,(k^+ + k_{IVR} - 2\,k_{EQ})}[1 - exp(-2\,k_{EQ}\,t)], \tag{5}$$

$$[\mathrm{LE_{IVR}}](t) = \frac{(k^+ - k_{EQ})}{(k^+ + k_{IVR} - 2\,k_{EQ})}[1 - exp(-(k^+ + k_{IVR})\,t)] - \frac{(k_{IVR} + k^+)}{2\,(k^+ + k_{IVR} - 2\,k_{EQ})}[1 - exp(-2\,k_{EQ}\,t)], \tag{6}$$

where [LE], [EXC], and [LE_{IVR}] represent the populations of the LE, EXC, and IVR states of the LE level, respectively; k^+, k_{IVR}, and k_{EQ} represent the rate constants of the EXC formation from the LE 6^1 level, the IVR rate of the LE level, and the equilibrium rate between the EXC and IVR states, respectively.

Physical Chemistry Chemical Physics Accepted Manuscript

Because we now know only the time evolution of the EXC state, all of the rate constants of the model cannot be determined at this stage. However, we can limit the range of the value by classifying the relations among the rate constants.

Case 1: Fast IVR ($k_{IVR} >> k^+$ and k_{EQ})

The first term of equation (5) decays rapidly, and the time evolution of the EXC state is proportional to $[1 - \exp(-2\ k_{EQ}\ t)]$; that is, only the equilibrium rate is effective. To match with the experimental result (τ = 10 ps), k_{EQ} should be 1/20 ps^{-1}, which is almost the same as the value for the 0^0 level. Because most of the excess energies remain within the reaction coordinate, a similar equilibrium rate to the EXC formation would be reasonable.

Case 2: Equal rate of IVR and EXC formation ($k_{IVR} = k^+$).

The second term, k_{EQ}, disappears due to the numerator, and the time evolution becomes proportional to $[1 - \exp(-(k_{IVR} + k^+)\ t)] = [1 - \exp(-2\ k^+\ t)]$. From the result of the 0^0 level, k^+ = 1/18 ps^{-1} was obtained. Therefore, 2 k^+ = 1/9 ps^{-1}, which closely matches the observed value. In this case, we cannot determine k_{EQ}.

Case 3: Slow IVR ($k_{IVR} << k_{EQ}$ and k^+).

This should not be the case, because the slow IVR rate means no vibration energy can be supplied into the reaction coordinate to accelerate the EXC formation rate. This contradicts the present experimental observation, but here we check the model. In this case, both terms of the equation (5) survive, and the time evolution of EXC is expressed by a bi-exponential form. This does not match with the experimental observation. To make the time dependence a single exponential function, both of the exponentials should match, i.e. $k^+ = 2\ k_{EQ}$ = 1/10 ps^{-1}. This contradicts with k^+ = 1/18 ps^{-1}, obtained from the reaction rate for the 0^0 level, and we can again rule out the slow IVR case.

It follows from these considerations that the supposed reaction scheme is reasonable to explain the experimental results. We can say that the IVR of the 6^1 level is faster than or comparable to the excimer formation, i.e. $k_{IVR} \geq k^+$ and k_{EQ}. The IVR rate of the 6^1 level of the Bz monomer is on the order of one hundred nanoseconds.[74-76] According to a stimulated Raman pumping study of Bz_2 in S_0, the IVR rate does not change according to the simple dimer formation.[31, 40] Thus, the IVR of Bz_2 in S_1, which is 3-orders faster than that of the monomer, is accelerated mainly by the EXC formation. The fast IVR may be stimulated by the reactive interaction and symmetry lowering in the EXC.

4-3. Relation to the structure

Saigusa and Lim reported that the EXC formation rates measured by the rise time of the EXC absorptions are not largely changed whether the cluster has the SW structure or not. This means that the SW structure is not always necessary for the appearance of the EXC absorption. A theoretical study on Bz_2^+ by Pieniazek *et al.* has shown that strong charge resonance absorptions appear even for the T-shape structure.[77, 78] Ion-pair states, which are expressed as linear combinations of states like $\phi_1^+\phi_2^-$, are also expected to contribute to stabilization of the EXC state. If the ion-pair states behave like the charge resonance state of Bz_2^+, the simple relation between EXC absorption and SW structure has some problem. The relation between the structure and the EXC absorption has already been considered based on time-resolved spectroscopy of a

Physical Chemistry Chemical Physics Accepted Manuscript

neat liquid of Bz. Miyasaka *et al.* have observed the time evolution of the transient absorption at 420 nm and 580 nm after one-photon excitation by 266 nm light, and reported similar time constants of 13 ± 1 ps for both wavelengths.[14] These time constants are in the middle of the present gas-phase results, 18 ps for 0^0 and 10 ps for 6^1. It is surprising that the EXC formation shows similar time constants in the gas and liquid phases. They ascribed this relatively slow reaction rate to extensive rearrangements of surrounding molecules in neat benzene during the course of the EXC formation process. In the gas phase, the structure just after excitation is T-shape, which needs the largest structural change to make the SW-shaped EXC. In the liquid phase, on the other hand, not all of the neighboring benzene has the T-shape contact. Thus, a much smaller structural change is sufficient to make the SW EXC and a faster EXC formation than the gas phase is expected. Thus, as they said, there is a possibility that in a neat liquid the appearance of the EXC absorption needs not only the association of excited and unexcited Bz molecules, but also some reorientation of the neighboring Bz molecules. To know much more about the relation between the cluster structure and the EXC formation dynamics, it is important to consider what kind of structure can show the EXC absorption.

4. Summary

We measured the real-time EXC formation dynamics of a gas-phase Bz_2 cluster after photo-excitation to the 0^0 and 6^1 (stem) levels. The time evolution of the EXC absorption shows a single exponential rise with time constants of 18 and 10 ps for the 0^0 and 6^1 levels, respectively. The time constant for the 0^0 level directly corresponds to the EXC formation time constant from the T-shape to the SW EXC. The IVR rate from the 6^1 level is estimated to be faster than, or similar to, the EXC formation by taking into account both the EXC formation and the IVR process from the 6^1 level. The EXC formation accelerates the IVR rate of the 6^1 level by more than one thousand times compared to that of the Bz monomer and the S_0 state of Bz_2.

Acknowledgement

The authors thank Prof. M. Sakai, Dr. S. Ishiuchi, and Dr. K. Misawa of Tokyo Institute of Technology as well as Prof. J. R. Woodward of the University of Tokyo for their helpful discussions. This work was supported in part by a Grant-in-Aid for Scientific Research KAKENHI in the innovative area 2503 and the Cooperative Research Program of the "Network Joint Research Center for Materials and Devices" from MEXT (Japan), and the Core-to-Core Program from Japan Society for Promotion of Science. M. M. also thanks for the supported from MEXT (Japan) through a project of the Grant-in-Aid for Young Scientists (B) (No. 21750013).

Physical Chemistry Chemical Physics Accepted Manuscript

Figures and captions

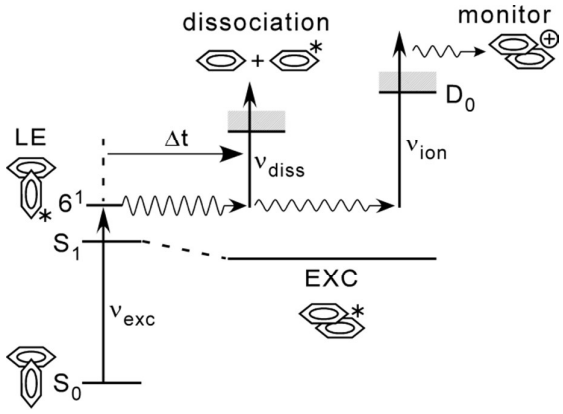

Figure 1 Excitation scheme of ionization-detected picosecond transient absorption. LE and EXC represent the locally excited states of the stem site and the excimer state, respectively. The ν_{diss} (21047 cm^{-1}, 2.6095 eV, 475 nm) is resonant with the dissociative EXC state composed of the S_3 excited state and the ground state benzenes. The ν_{ion} (37026 cm^{-1}, 4.5907 eV, 270 nm) is introduced few tenths of a nanosecond after the excitation, ν_{exc}.

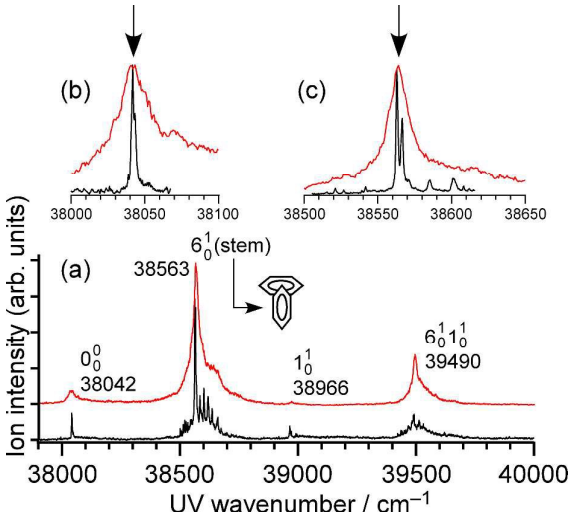

Figure 2 Resonance enhanced 2 photon ionization spectra of the benzene dimer (Bz_2). The upper (red) and lower (black) traces in each figure show the spectra obtained when using picosecond and nanosecond lasers, respectively. Spectra in (b) and (c) show expanded views with a slower scan rate around the 0^0_0 and 6^1_0 bands, respectively. The arrows in (b) and (c) indicate the positions of excitation in the time evolution measurement.

Physical Chemistry Chemical Physics Accepted Manuscript

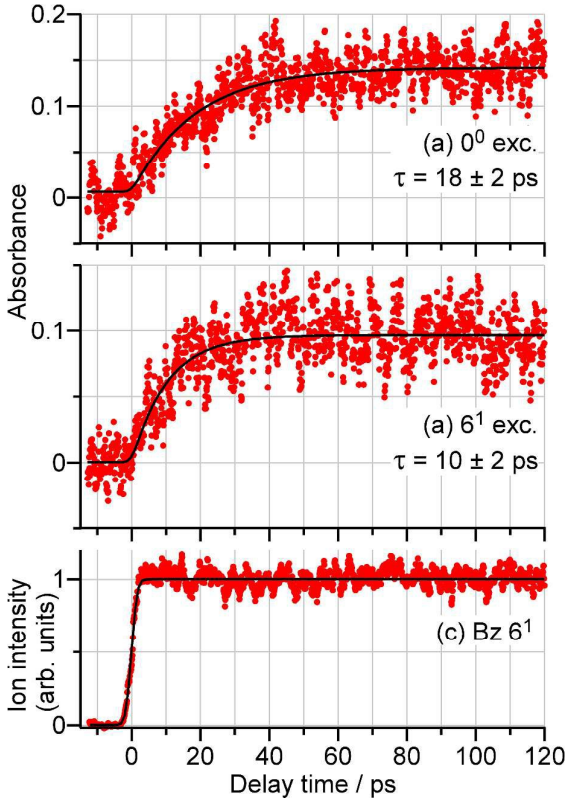

Figure 3 Time profiles of the EXC absorption of benzene dimer (Bz_2) obtained by exciting (a) the 0^0 and (b) the 6^1 levels (dots). The probe wavelength is 475 nm for each. The time profile in (c) shows the time evolution of the 1+2' multi-photon ionization of the 6^1 level of bare benzene, which approximately represents the instrumental function (see text). The black curve on each profile shows a single exponential function obtained by a fitting. The time constants are also indicated.

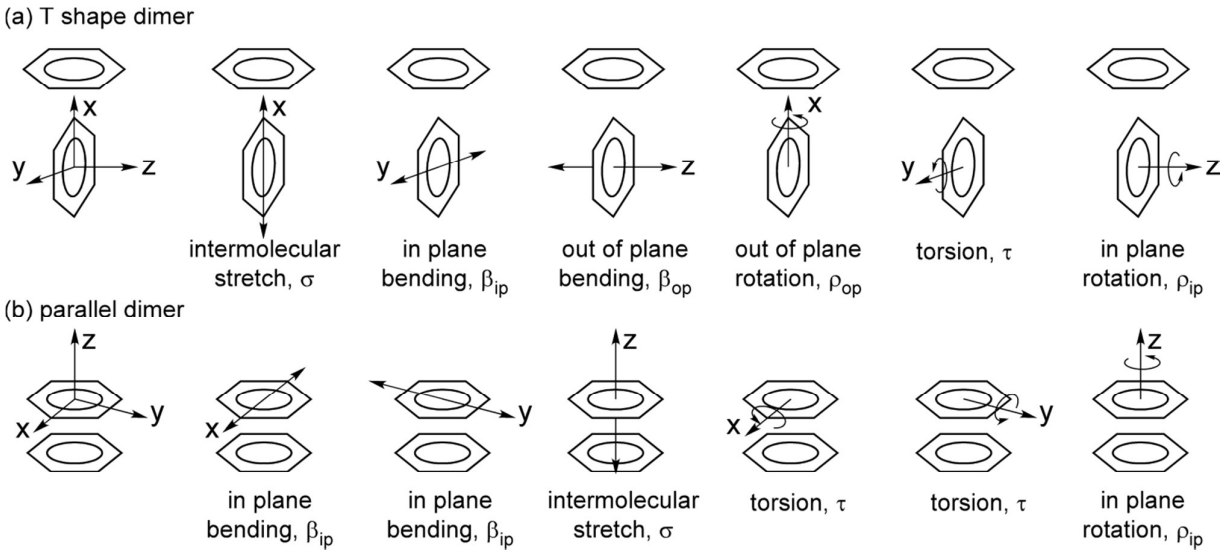

Figure 4 Schematic pictures of the structure and intermolecular vibrations of (a) T- and (b) parallel-shaped benzene dimer (Bz_2). The intermolecular vibrations are represented by the motions of one benzene ring, and the other ring is fixed for simplicity, though both of the rings should move so as to

Physical Chemistry Chemical Physics Accepted Manuscript

conserve the center of mass. The coordinate axes are fixed on the moving ring, and are labeled based on the monomer system.

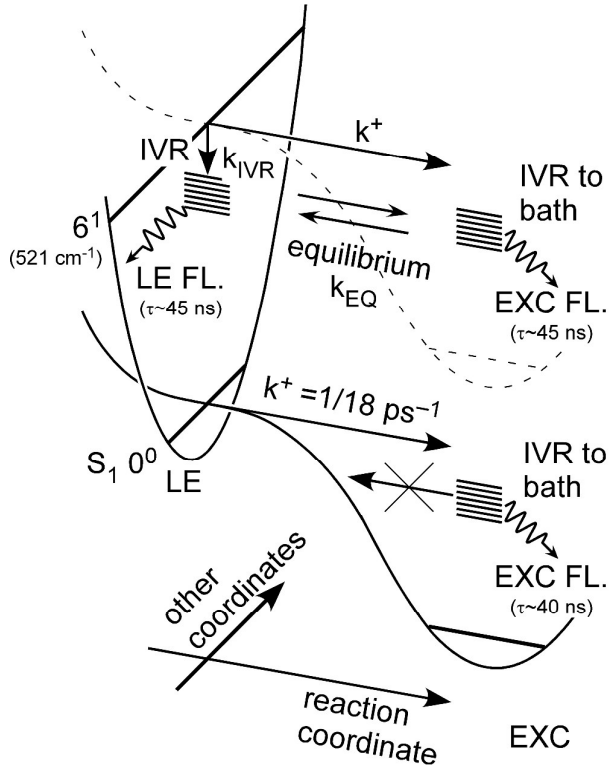

Figure 5 Schematic diagram of the excimer (EXC) formation reaction in the S_1 state of the benzene dimer (Bz_2). LE and EXC represent the locally excited state of the stem site and EXC state, respectively. The reaction coordinate means EXC formation and other coordinates are orthogonal to this. This figure shows, as a representative, mode 6 of the stem site. Bath, which is not vibrations on the reaction coordinate, contains all of the intermolecular coordinates other than the reaction coordinate.

Physical Chemistry Chemical Physics Accepted Manuscript

Table of Contents Entry

Photoexcitation of T-shaped benzene dimer provides sandwiched excimer in 10 ps accompanying 1000 times faster intracluster vibrational energy redistribution rate than the benzene monomer.

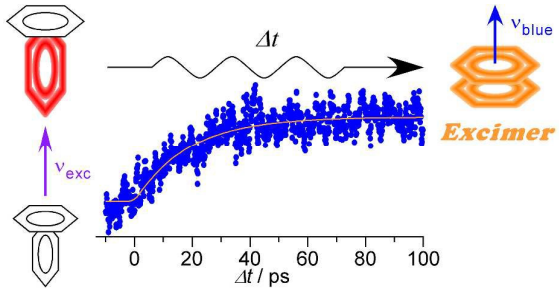

Physical Chemistry Chemical Physics Accepted Manuscript

References

1. Ch. K. Rhodes, *Excimer Lasers*, Springer, 1979.
2. J. B. Birks, *Rep. Prog. Phys.*, 1975, **38**, 903-974.
3. J. B. Birks, *Nature*, 1967, **214**, 1187-1190.
4. P. Conlon, C. J. Yang, Y. Wu, Y. Chen, K. Martinez, Y. Kim, N. Stevens, A. A. Marti, S. Jockusch, N. J. Turro and W. Tan, *J. Am. Chem. Soc.*, 2008, **130**, 336-342.
5. T. Costa, J. Sergio Seixas de Melo, C. S. Castro, S. Gago, M. Pillinger and I. S. Goncalves, *J. Phys. Chem. B*, 2010, **114**, 12439-12447.
6. K. Yoshihara, T. Kasuya, A. Inoue and S. Nagakura, *Chem. Phys. Lett.*, 1971, **9**, 469-472.
7. R. Seyfang, E. Betz, H. Port, W. Schrof and H. C. Wolf, *Journal of Luminescence*, 1985, **34**, 57-62.
8. R. Seyfang, H. Port and H. C. Wolf, *Journal of Luminescence*, 1988, **42**, 127-135.
9. R. Seyfang, H. Port, P. Fischer and H. C. Wolf, *Journal of Luminescence*, 1992, **51**, 197-208.
10. R. B. Pansu, K. Yoshihara, T. Arai and K. Tokumaru, *J. Phys. Chem.*, 1993, **97**, 1125-1133.
11. N. Nakashima, M. Sumitani, I. Ohmine and K. Yoshihara, *J. Chem. Phys.*, 1980, **72**, 2226-2230.
12. Y. Inokuchi, Y. Naitoh, K. Ohashi, K.-i. Saitow, K. Yoshihara and N. Nishi, *Chem. Phys. Lett.*, 1997, **269**, 298-304.
13. A. Waldman and S. Ruhman, *Chem. Phys. Lett.*, 1993, **215**, 470-476.
14. H. Miyasaka, H. Masuhara and N. Mataga, *J. Phys. Chem.*, 1985, **89**, 1631-1636.
15. N. Nakashima, H. Inoue, M. Sumitani and K. Yoshihara, *J. Chem. Phys.*, 1980, **73**, 5976-5980.
16. L. R. Williams and K. A. Nelson, *J. Chem. Phys.*, 1987, **87**, 7346-7347.
17. H. Masuhara, H. Miyasaka, N. Ikeda and N. Mataga, *Chem. Phys. Lett.*, 1981, **82**, 59-62.
18. J. N. Schrauben, J. L. Ryerson, J. Michl and J. C. Johnson, *J. Am. Chem. Soc.*, 2014, **136**, 7363-7373.
19. H. L. Stern, A. J. Musser, S. Gelinas, P. Parkinson, L. M. Herz, M. J. Bruzek, J. Anthony, R. H. Friend and B. J. Walker, *Proc. Natl. Acad. Sci. USA*, 2015, **112**, 7656-7661.
20. B. J. Walker, A. J. Musser, D. Beljonne and R. H. Friend, *Nat Chem*, 2013, **5**, 1019-1024.
21. P. M. Zimmerman, Z. Zhang and C. B. Musgrave, *Nat Chem*, 2010, **2**, 648-652.
22. W. T. Simpson and D. L. Peterson, *J. Chem. Phys.*, 1957, **26**, 588-593.
23. A. Witkowski and W. Moffitt, *J. Chem. Phys.*, 1960, **33**, 872-875.
24. R. L. Fulton and M. Gouterman, *J. Chem. Phys.*, 1961, **35**, 1059-1071.
25. R. L. Fulton and M. Gouterman, *J. Chem. Phys.*, 1964, **41**, 2280-2286.
26. A. Eisfeld, L. Braun, W. T. Strunz, J. S. Briggs, J. Beck and V. Engel, *J. Chem. Phys.*, 2005, **122**, 134103.
27. M. Andrzejak and P. Petelenz, *Chem. Phys.*, 2007, **335**, 155-163.
28. H. Saigusa and E. C. Lim, *J. Phys. Chem.*, 1990, **94**, 2631-2637.
29. K. Diri and A. I. Krylov, *J. Phys. Chem. A*, 2012, **116**, 653-662.

Physical Chemistry Chemical Physics Accepted Manuscript

30. V. Špirko, O. Engkvist, P. Soldán, H. L. Selzle, E. W. Schlag and P. Hobza, *J. Chem. Phys.*, 1999, **111**, 572-582.
31. S. Tsuzuki, T. Uchimaru, K.-i. Sugawara and M. Mikami, *J. Chem. Phys.*, 2002, **117**, 11216-11221.
32. M. O. Sinnokrot and C. D. Sherrill, *J. Phys. Chem. A*, 2006, **110**, 10656-10668.
33. J. G. Hill, J. A. Platts and H.-J. Wrner, *Phys. Chem. Chem. Phys.*, 2006, **8**, 4072-4078.
34. E. C. Lee, D. Kim, P. Jurečka, P. Tarakeshwar, P. Hobza and K. S. Kim, *J. Phys. Chem. A*, 2007, **111**, 3446-3457.
35. I. V. Hertel and W. Radloff, *Rep. Prog. Phys.*, 2006, **69**, 1897-2003.
36. L. R. Khundkar and A. H. Zewail, *Annu. Rev. Phys. Chem.*, 1990, **41**, 15-60.
37. H. Saigusa and E. C. Lim, *Chem. Phys. Lett.*, 2001, **336**, 65-70.
38. E. Arunan and H. S. Gutowsky, *J. Chem. Phys.*, 1993, **98**, 4294-4296.
39. T. Ebata, M. Hamakado, S. Moriyama, Y. Morioka and M. Ito, *Chem. Phys. Lett.*, 1992, **199**, 33-41.
40. B. F. Henson, G. V. Hartland, V. A. Venturo and P. M. Felker, *J. Chem. Phys.*, 1992, **97**, 2189-2208.
41. V. A. Venturo and P. M. Felker, *J. Chem. Phys.*, 1993, **99**, 748-751.
42. P. M. Felker, P. M. Maxton and M. W. Schaeffer, *Chem. Rev.*, 1994, **94**, 1787-1805.
43. M. W. Schaeffer, P. M. Maxton and P. M. Felker, *Chem. Phys. Lett.*, 1994, **224**, 544-550.
44. W. Scherzer, O. Krätzschmar, H. L. Selzle and E. W. Schlag, *Z. Naturforsch.*, 1992, **47 a**, 1248-1252.
45. H. Shinohara and N. Nishi, *J. Chem. Phys.*, 1989, **91**, 6743-6751.
46. W. Radloff, V. Stert, T. Freudenberg, I. V. Hertel, C. Jouvet, C. Dedonder-Lardeux and D. Solgadi, *Chem. Phys. Lett.*, 1997, **281**, 20-26.
47. T. Hirata, H. Ikeda and H. Saigusa, *J. Phys. Chem. A*, 1999, **103**, 1014-1024.
48. H. Saigusa, M. Morohoshi and S. Tsuchiya, *J. Phys. Chem. A*, 2001, **105**, 7334-7340.
49. J. C. Amicangelo, *J. Phys. Chem. A*, 2005, **109**, 9174-9182.
50. G. Olaso-González, D. Roca-Sanjuán, L. Serrano-Andrés and M. Merchán, *J. Chem. Phys.*, 2006, **125**, 231102.
51. T. Rocha-Rinza, L. D. Vico, V. Veryazov and B. O. Roos, *Chem. Phys. Lett.*, 2006, **426**, 268-272.
52. R. Huenerbein and S. Grimme, *Chem. Phys.*, 2008, **343**, 362-371.
53. R. F. Fink, J. Pfister, H. M. Zhao and B. Engels, *Chem. Phys.*, 2008, **346**, 275-285.
54. T. Rocha-Rinza and O. Christiansen, *Chem. Phys. Lett.*, 2009, **482**, 44-49.
55. F. Hirayama, *J. Chem. Phys.*, 1965, **42**, 3163-3171.
56. J. B. Hopkins, D. E. Powers and R. E. Smalley, *J. Phys. Chem.*, 1981, **85**, 3739-3742.
57. O. Krätzschmar, H. L. Selzle and E. W. Schlag, *J. Phys. Chem.*, 1994, **98**, 3501-3505.
58. R. Cooper and J. K. Thomas, *J. Chem. Phys.*, 1968, **48**, 5097-5102.
59. J. K. Thomas and I. Mani, *J. Chem. Phys.*, 1969, **51**, 1834-1838.
60. S. Ishiuchi, K. Daigoku, M. Saeki, M. Sakai, K. Hashimoto and M. Fujii, *J. Chem. Phys.*, 2002, **117**, 7077-7082.

Physical Chemistry Chemical Physics Accepted Manuscript

61. S. Ishiuchi, K. Daigoku, M. Saeki, M. Sakai, K. Hashimoto and M. Fujii, *J. Chem. Phys.*, 2002, **117**, 7083-7093.
62. P. R. R. Langrldge-Smith, D. V. Brumbaugh, C. A. Haynam and D. H. Levy, *J. Phys. Chem.*, 1981, **85**, 3742-3746.
63. K. S. Law, M. Schauer and E. R. Bernstein, *J. Chem. Phys.*, 1984, **81**, 4871-4882.
64. K. O. Börnsen, H. L. Selzle and E. W. Schlag, *J. Chem. Phys.*, 1986, **85**, 1726-1732.
65. T. A. Stephenson, P. L. Radloff and S. A. Rice, *J. Phys. Chem.*, 1984, **81**, 1060-1072.
66. T. Omi, H. Shitomi, N. Sekiya, K. Takazawa and M. Fujii, *Chem. Phys. Lett.*, 1996, **252**, 287.
67. T. Iimori and Y. Ohshima, *J. Chem. Phys.*, 2001, **114**, 2867-2870.
68. T. Iimori and Y. Ohshima, *J. Chem. Phys.*, 2002, **117**, 3656-3674.
69. T. Iimori and Y. Ohshima, *J. Chem. Phys.*, 2002, **117**, 3675-3686.
70. M. Miyazaki and M. Fujii, **to be published**.
71. E. Riedle, T. Knittel, T. Weber and H. J. Neusser, *J. Chem. Phys.*, 1989, **91**, 4555-4563.
72. M. Yamawaki, Y. Tatamitani, A. Doi, S. Kasahara and M. Baba, *J. Mol. Spectros.*, 2006, **238**, 49-55.
73. S. Thorwirth, P. Theulé, C. A. Gottlieb, M. C. McCarthy and P. Thaddeus, *Astrophys. J.*, 2007, **662**, 1309-1314.
74. T. A. Stephenson and S. A. Rice, *J. Chem. Phys.*, 1984, **81**, 1073-1082.
75. J. B. Hopkins, D. E. Powers and R. E. Smalley, *J. Chem. Phys.*, 1980, **72**, 5039-5048.
76. J. B. Hopkins, D. E. Powers, S. Mukamel and R. E. Smalley, *J. Chem. Phys.*, 1980, **72**, 5049-5061.
77. P. A. Pieniazek, A. I. Krylov and S. E. Bradforth, *J. Chem. Phys.*, 2007, **127**, 044317.
78. P. A. Pieniazek, S. E. Bradforth and A. I. Krylov, *J. Chem. Phys.*, 2008, **129**, 074104.

Physical Chemistry Chemical Physics Accepted Manuscript